Scalability of quantum computing based on nanomechanical resonators

Li-gong Zhou (周利功), Ming Gao (高明), Jin-lin Peng (彭金林), and Xiang-bin Wang (王向斌)

Scalable quantum computing with switchable nanomechanical-resonator interactions

Li-gong Zhou (周立功),[1] Ming Gao (高明),[1, 2] Jin-lin Peng (彭进霖),[1, 3] and Xiang-bin Wang (王向斌)[1, 4, *]

[1]*State Key Laboratory of Low Dimensional Quantum Physics,*
Tsinghua University, Beijing 100084, People's Republic of China
[2]*Department of Physics, National University of Defense Technology, Changsha 410073, People's Republic of China*
[3]*School of Electronic and Electrical Engineering University of Leeds, Leeds, UK*
[4]*Shandong Academy of Information & Communication Technology, Jinan 250101, People's Republic of China*

We study scalability of quantum computing based on nanomechanical resonator (NAMR), including the consequences of the effective next-nearest spin-spin couplings induced by the NAMRs, NAMR frequency errors, and NAMR-spin coupling errors on the scalability of quantum computing based on NAMRs. We show the fidelity change of the quantum operation due to these errors numerically. Switchable interactions between NAMRs can be achieved by adding control gates. Based on this modification, we present a method to perfectly avoid the next-nearest spin-spin couplings and compensate for the negative effects due to the frequency errors and spin coupling errors.

I. INTRODUCTION

Scalability is one of the most important issues in the realization of quantum computing. For example, in order to factorize a 200-digit number using a quantum computer, one needs to manipulate thousands of qubits [1]. However, in realistic physical systems, there are many imperfections, such as the quantum decoherence, the device errors, and so on. These imperfections seriously limit the power of a quantum computing device. In particular, in a large scale quantum computing, the small error of each individual device can accumulate and this may lead to the failure of the final result [2].

In recent years, methods for scalable quantum computing based on artificial quantum systems have been extensively studied [1, 3–6]. A promising scalable quantum computing architecture based on spin system of NAMRs was proposed by P. Rabl *et. al.* [6]. The spins have a long decoherence time and the NAMRs can be fabricated on a large scale. The quantum motions of the NAMRs can strongly interact with the spins [7] and induce strong couplings between the spins [6, 8, 9].

However, the fact is that various kinds of errors inevitably exist in realistic systems, e.g., the next-nearest interactions between the spins induced by the NAMRs [6], the frequency errors of the NAMRs (about $\pm 1.0\%$ deviations from the averaged frequency was experimentally shown by E. Buks in Ref. [10]), the coupling fluctuations between the NAMRs and the coupling fluctuations between an NAMR and the corresponding spin qubit. These intrinsic and device errors inevitably fluctuate the effective interactions between the spins. These errors (we mean the next-nearest spin-spin interactions and the device errors, similarly hereinafter.) cause the actual state deviating from the target state and finally reduce the quality of the quantum gate and limit the

scalability of the system. These quantum imperfections may cause exponential suppression of quantum computations [11]. Thus it is an important issue to find out quantitatively the impacts of these errors and the efficient method to avoid or compensate for the significant negative effects.

In this article, we consider a scalable quantum computing architecture consisting of N spin qubits whose interactions are mediated by an array of N NAMRs [6]. The device errors of the NAMRs shift the frequencies of the collective modes, the NAMR-spin coupling strengths and result in fluctuations in the effective spin-spin couplings. For a given evolution time, the spins' final state depends on the coupling strengths among them. Supposing a certain duration is needed as the right evolution time to produce the target state in the ideal case of no errors, the same evolution will produce a wrong state in the actual case with errors. Here, we analyze the impacts of these errors on the quantum operation fidelity. The simulation results suggest that the next-nearest spin-spin couplings and the device errors are very devastating for the scalability. Based on the analysis, we propose a method to compensate for these negative effects. Meanwhile by adding control gates between them to generate switchable interactions, this method can also avoid the effective next-nearest spin-spin couplings.

This article is arranged as follows: In Sec. II we review the model discussed in this article. Next, we give the consequence of the influences of the next-nearest interactions in Sec. III and the device errors in Sec. IV on quantum operation fidelity by numerical simulations. We study how the influences of these errors change with the number of the NAMRs N. In Sec. V we present our theoretical method to avoid the next-nearest couplings and simultaneously resist the device errors. Finally, we present discussions and conclusions in Sec. VI. The method of diagonalizing the quadratic boson Hamiltonian are appended in the appendix.
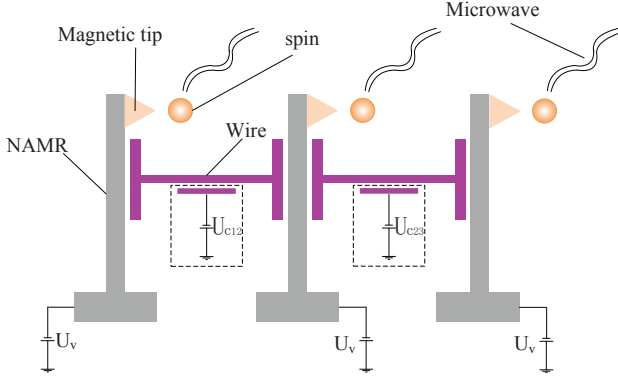
*Electronic address: xbwang@mail.tsinghua.edu.cn

FIG. 1: (Color online.) Switchable coupling between two NAMRs. A switchable control gate (dashed box) is added between every two nearest NAMRs.

II. MODEL

We consider a system consisting of an array of N NAMRs, which are charged and interact capacitively with nearby wires interconnecting them [6]. A magnetic tip is attached on the free end of each NAMR. An NAMR with fundamental frequency ω_i and effective mass m magnetically couples to an electronic spin qubit associated with a nitrogen-vacancy (N-V) center [7, 12]. Each spin is driven by a local microwave to form a pair of dressed states in order to match the NAMR frequency [7]. The interaction Hamiltonian between the NAMR and the corresponding spin qubit is $H_{\mathrm{sr}}^i = \frac{\lambda_i}{2}(a_i^\dagger + a_i)\sigma_z^i$ [6]. Here $a_i^\dagger$ (a_i) is the natural creation (annihilation) operator of the fundamental vibrational mode of the ith NAMR and σ_z^i is the Pauli-z operator of the ith spin. The coupling strength $\lambda_i = g_s\mu_B G_m a_{0i}/\hbar$ with $g_s = 2$, the Bohr magneton μ_B, the magnetic field gradient G_m and the amplitude of zero-point fluctuations $a_{0i} = \sqrt{\hbar/(2m\omega_i)}$.

The Hamiltonian of these N coupled NAMRs is (setting $\hbar = 1$) [6]:

$$H_{\mathrm{ph}} = \sum_{i=1}^N \omega_i a_i^\dagger a_i + \frac{1}{2}\sum_{i,j}^N g_{i,j}(a_i + a_i^\dagger)(a_j + a_j^\dagger), \quad (1)$$

with $g_{i,j}$ is the coupling between the ith NAMR and the jth NAMR. The derivation details of $g_{i,j}$ can be found in the appendix. The interaction $g_{i,j}$ consists of two parts: the self-coupling $g_{i,i}$ and the coupling between different NAMRs $g_{i,j}$ ($i \neq j$). The first item of H_{ph} is the free Hamiltonian of the NAMRs and the second item is sum of the interactions among them.

The Hamiltonian H_{ph} can be diagonalized by defining collective modes, the total NAMR-spin coupling Hamiltonian (the sum of H_{sr}^i over i) can be rewritten as the coupling between the z-components of the electronic spins and the collective modes of the NAMRs. After a transformation, the effective spin-spin interactions mediated

by the NAMRs can be obtained

$$H_{\mathrm{eff}} = \sum_{i,j} M_{i,j}\sigma_z^i\sigma_z^j, \quad (2)$$

with $M_{i,j}$ the effective coupling strength between the spin i and the spin j, which could be used for scalable quantum computation [6].

We consider an array of Si-NAMRs with typical parameters: NAMR frequency $\omega_r/(2\pi)$ varies from 1.0 MHz to 5.0 MHz, $a_0 \approx 1.86 \times 10^{-13}$ m and $g/(2\pi) = 500$ kHz [6]. For gradient $G_m = 9.6 \times 10^6$ Tm^{-1}, the resulting coupling strength between an NAMR with frequency ω_r and a spin is about $\lambda/(2\pi) \approx 50$ kHz. In this case, the effective nearest neighbour spin-spin coupling is about a few kilohertz.

III. NEXT-NEAREST SPIN-SPIN COUPLINGS

Based on the model above, we analysize the effects of the next-nearest spin-spin interactions and the device errors. We shall calculate the fidelity of the *target state* from the ideal model without any errors and the *actual state* from the more realistic model with independent errors.

From equation (2) we know that the NAMRs induce next-nearest and higher order interactions between spins, which lead to deviation from the target state. The next-nearest interactions are intrinsic and dependent on the nature of the quantum computation architecture. These destructive interactions can't be eliminated by improving the preparation technologies and lead to the decrease of the quantum gate quality. The interactions between the spins are $M_{i,i+m} \sim (g/\omega_r)^{m-1}$ in the regime of $(g/\omega_r) \ll 1$ [6]. But the smaller the (g/ω_r) is, the weaker the effective nearest spin-spin coupling is. The value of (g/ω_r) can't be too small if we want to obtain strong enough nearest spin-spin coupling to complete a quantum gate. Thus, the effect of these next-nearest couplings should be studied quantitatively.

In the case of ideal situation, the coupling between the spins can be described by Ising model and the coupling strength between the nearest spins is denoted by M. For N NAMRs with an initial state $|\psi_{\mathrm{in}}\rangle = [(|0\rangle + |1\rangle)/\sqrt{2}]^{\otimes N}$. We choose the evolution time

$$t_g = (2N-1)\pi/(4M), \quad (3)$$

then the produced state is in the following form

$$|\psi_o(N, \{j = \pm 1\})\rangle = \frac{1}{2^{N/2}}\bigotimes_{j=1}^N \left(|0\rangle\sigma_z^{j+1} + |1\rangle\right), \quad (4)$$

with the convention $\sigma_z^{N+1} = 1$, which is equivalent to the 1-D cluster state [13, 14]. In the realistic case, the spins' state is $|\phi_o(N, \{j\})\rangle = U_g(t_g)|\psi_{\mathrm{in}}\rangle$ with $U_g(t_g)$ the evolution operator within time t_g. The fidelity between
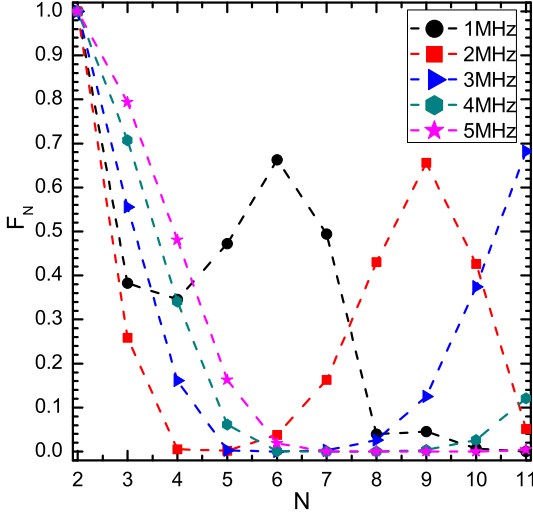
FIG. 2: (Color online.) The influences of next-nearest spin-spin interactions on quantum information processing with different NAMR frequencies. For $N = 2$, the fidelity $F = 1$ since there is no next-nearest spin-spin interactions. Here the NAMR-NAMR coupling $g/(2\pi) = 500$ kHz and the NAMR frequencies are given in the legend.

the state with only nearest and next-nearest interactions and the *target state* with only nearest interactions is

$$F(N) = |\langle\phi_\mathrm{o}(N, \{j = i \pm 1, i \pm 2\})|\phi_\mathrm{o}(N, \{j = i \pm 1\})\rangle|. \quad (5)$$

For example, for $N = 2$, the evolution time should be chosen as $t_\mathrm{g} = \pi/(4|M|)$ [6], which is within the spin decoherence time and the dephasing time. For example, the spin decoherence time $T_2 \approx 6$ ms [15] and the dephasing time induced by nuclear-spin fluctuations $T_2' \approx 0.35$ ms for N-V centers [16] are observed experimentally.

The simulation results are shown in Fig. 2 with different NAMR frequencies. This figure suggests that when the NAMR-NAMR coupling g is comparable with the NAMR frequency ω_r, the next-nearest spin-spin interactions are ignorable. This shows that, as the number of qubits increases, the errors in the target state rise, hence one may end up with a wrong result with large probability in a large scale quantum computation.

Fig. 2 also suggests that the fidelity F oscillates with the increasing of NAMR-spin block number N for a fixed NAMR frequency. The fidelity F oscillates slower for larger NAMR frequency. These fidelity oscillations are due to the effective next-nearest spin-spin interaction induced by the NAMRs and can be physically understood as follows. The fidelity "phase shift" is induced by the effective next-nearest spin-spin interactions and becomes larger and larger as the number of the NAMR-spin blocks increases. The fidelity comes back when the "phase shift" runs up to 2π with a smaller value for the propagation of error. For larger NAMR frequency, the effective next-nearest spin-spin interactions are weak comparing with the nearest spin-spin interactions. Thus, the 2π "phase

shift" needs more NAMR-spin blocks and the oscillation period appears larger comparing with that of smaller NAMR frequency case.

IV. DEVICE ERRORS

Besides the intrinsic next-nearest spin-spin interactions, there are also many other device errors due to imperfect preparation processes. Here, we focus on the NAMRs' frequency errors, NAMR-NAMR coupling errors and NAMR-spin coupling errors, which can be compensated for by the proposal given in Sec. V.

Frequency errors. Denoting the frequency of each NAMR $\omega_i = \omega_\mathrm{r} + \epsilon_i$ with ω_r the averaged frequency of all the NAMRs and ϵ_i the frequency error, the coupling strength between the NAMR and the corresponding spin can be written as

$$\lambda_i = \lambda\sqrt{\frac{\omega_\mathrm{r}}{\omega_i}}, \quad (6)$$

which means that the frequency errors generally fluctuate the NAMR-spin couplings. The NAMR-spin coupling in the form of collective operators can be rewritten as

$$\sum_i^N \frac{\lambda_i}{2}(a_i + a_i^\dagger)\sigma_z^i = \sum_{n,i=1}^N \lambda_{n,i}(b_n + b_n^\dagger)\sigma_z^i, \quad (7)$$

with

$$\lambda_{n,i} = \lambda_i(J_{i,n}^{-1} + J_{i,n+N}^{-1}), \quad (8)$$

the coupling strength between the nth collective mode and the z component of the ith spin (The method of diagonalizing this Hamiltonian is given in the appendix). Here $\{J_{i,j}^{-1}\}$ are the matrix elements of J^{-1}. Therefore the effective spin-spin coupling is $M_{i,j} = \sum_n \lambda_{n,i}\lambda_{n,j}/(4\tilde\omega_n)$ with $\tilde\omega_n$ the collective frequencies and $b_n^\dagger$ the corresponding creation operators. The collective frequencies are shifted by the frequency errors and the numerically result for $N = 11$ is as shown in Fig. 3.

For N NAMRs with an initial state $|\psi_\mathrm{in}\rangle = [(|0\rangle + |1\rangle)/\sqrt{2}]^{\otimes N}$, the relative frequency errors are denoted by $\Delta_i = \varepsilon_i/\omega_\mathrm{r}$. After some appropriate time t_g (determined by N), the spins' state becomes $|\phi_\mathrm{o}(N, \{\Delta_i\})\rangle = U_\mathrm{g}(t_\mathrm{g})|\psi_\mathrm{in}\rangle$. The fidelity between the state with frequency errors only and the *target state* (without next-nearest spin-spin interactions or any other errors) is

$$F(N, \{\Delta_i\}) = |\langle\phi_\mathrm{o}(N, \{\Delta_i\})|\phi_\mathrm{o}(N, \{\Delta_i = 0\})\rangle|. \quad (9)$$

We consider the NAMRs given in Sec. II. Our numerical simulations show that the fidelity $F(N, \{\Delta_i\})$ decreases with the growth of N, as sketched in Fig. 4. The Fig. 4 gives $F(2, \Delta_\mathrm{m} = 1.0\%) \approx 0.9997$ while $F(11, \Delta_\mathrm{m} = 1.0\%) \approx 0.9475$; and $F(2, \Delta_\mathrm{m} = 5.0\%) \approx 0.9944$ while $F(11, \Delta_\mathrm{m} = 5.0\%) \approx 0.2757$. Here $F(N, \Delta_\mathrm{m} = 5.0\%)$ is the value for $F(N, \{\Delta_i\})$ where the
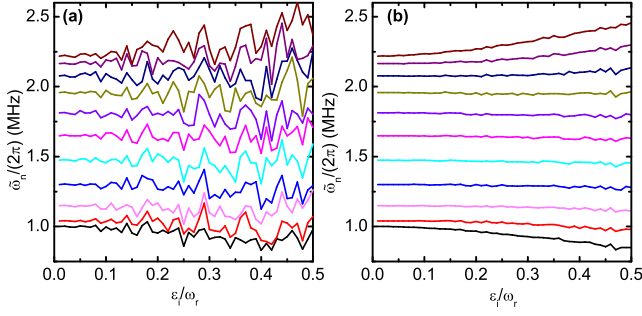
FIG. 3: (Color online.) The collective frequencies of the NAMRs are shifted by their random frequency errors for $N = 11$ with numerical calculations. The parameters used here are: $\omega_r/(2\pi) = 1$ MHz, the coupling strength: $g/(2\pi) = 500$ kHz. The left panel (a) is the result by running the program one time while the right panel (b) is the average by running the program 200 times. The offsets of the collective frequencies are optimistic estimations.

FIG. 5: (Color online.) The fidelity F decreases as the number of the NAMRs N increases with (a) only λ_i errors and (b) only $g_{i,i+1}$ errors. The errors compared with the central values are: 1.0%, 3.0%, and 5.0%. The results are averaged by running the program 200 times. Here $\omega_r/(2\pi) = 1$ MHz and the averaged NAMR-NAMR coupling $g/(2\pi) = 500$ kHz.
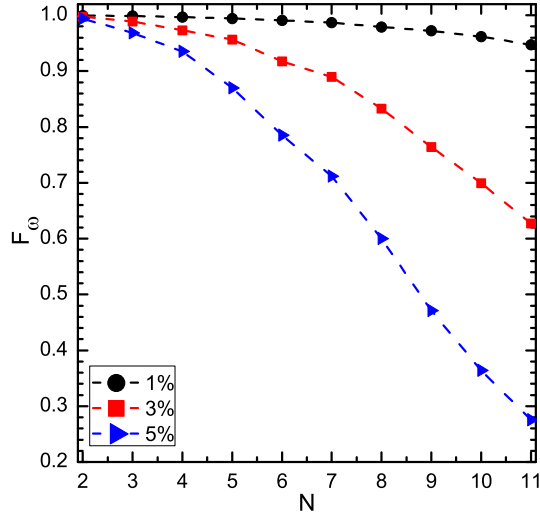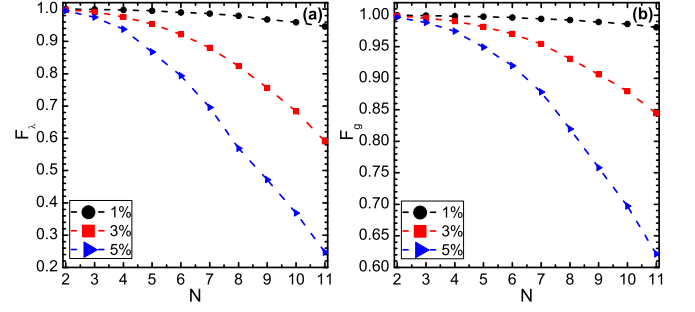

FIG. 4: (Color online.) The fidelity F decreases as the number of the NAMRs N increases (we run the program 200 times for average to get the tendency of the fidelity). The frequency errors compared with the central frequency are: 1.0% , i.e., $\Delta_m = 1.0\%$ and the same below, 3.0% , and 5.0%.

consider the nearest NAMR-NAMR interactions [6]. The interactions between nearest NAMRs can't be exactly the same in practice and denoted by $g_{i,i}$ and $g_{i,i+1} = g_{i+1,i}$. The matrix A and B (see the appendix) are given by

$$A = B + \text{diag}\left(\frac{\omega_1}{2}, \frac{\omega_2}{2}, \cdots, \frac{\omega_N}{2}\right), \tag{10a}$$

$$B = \begin{bmatrix} \frac{1}{2}g_{1,1} & \frac{1}{2}g_{1,2} & & & \\ \frac{1}{2}g_{2,1} & g_{2,2} & \frac{1}{2}g_{2,3} & & \\ & \ddots & \ddots & \ddots & \\ & & \frac{1}{2}g_{N-1,N-2} & g_{N-1,N-1} & \frac{1}{2}g_{N-1,N} \\ & & & \frac{1}{2}g_{N,N-1} & \frac{1}{2}g_{N,N} \end{bmatrix}_{N\times N} . \tag{10b}$$

The effects of the NAMR-NAMR coupling fluctuations on the fidelity between the *actual state* with only $g_{i,i+1}$ errors of different amplitudes and the *target state* are shown in Fig. 5 (b) by numerical simulations.

V. COMPENSATION METHOD

As analyzed above, the device errors (e.g., frequency errors) lead to fidelity decease of the quantum operation. The infidelity cannot be compensated by simply adjusting the evolution time t_g when $N > 2$, as shown in Fig. 6. In what follows, we propose a method to solve this problem. The main idea is that the device errors can be perfectly compensated for by controlling the interaction time of each two adjacent spin qubits block. With this compensation method, one can produce arbitrarily large-scale states with whatever large device error of each NAMR. In addition, this method also avoid the effective next-nearest spin-spin couplings.

values of each Δ_i are randomly chosen from the range $[-\Delta_m, +\Delta_m]$.

Errors of λ_i. The expression of λ_i [see eq. (6)] suggests that the NAMR-spin coupling strength depends on the NAMR's frequency ω_i and the coupling constant λ, which is dependent on the magnetic moment of the tip, the position of the spin and so on. We can reduce these device errors to the NAMR-spin coupling fluctuations. The influences of these device errors on quantum gate also should be studied. The fidelity between the *actual state* with only λ_i errors of different amplitudes and the *target state* is simulated as shown in Fig. 5 (a).

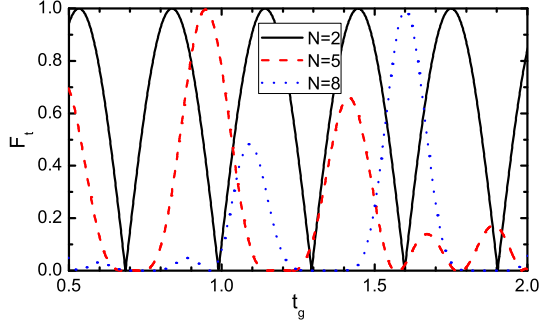*Errors of $g_{i,i\pm1}$.* For the system we considered, we only

FIG. 6: (Color online.) The fidelity F changes as a function of the evolution time t_g with only frequency errors. Here F denotes the fidelity between the target state and the actual state at an arbitrary time t_g. These curves suggest that the infidelity $(1-F)$ caused by frequency errors can't be compensated for by only adjusting the evolution time t_g when $N > 2$. In this figure, the frequency errors are within 1.0% compared with ω_r. The black (solid) curve is for $N = 2$, the dashed (red) curve is for $N = 5$ and the dotted (blue) curve is for $N = 8$.

A. Switchable nearest NAMR-NAMR coupling

For a one-dimensional N NAMR-spin chain, an auxiliary switchable control voltage gate is added between every two nearest NAMRs to obtain switchable coupling between them, as depicted in Fig. 1. When the control voltage U_{c12} is zero, the nearest NAMRs couple with each other and induce effective spin-spin interactions; and when the control voltage U_{c12} is switched on and equals to the NAMR's gate voltage U_v, the coupling of the two NAMRs connected this gate is switched off, hence the NAMRs induce no effective spin-spin interactions. The effective coupling strength between every two nearest spins in the case of device errors can be theoretically measured and denoted by $M_{i,i\pm1}$ by assuming that the other NAMRs and spins do not exist.

The Hamiltonian for coupled NAMRs is

$$H_p = \sum_i \frac{p_i^2}{2m_r} + \frac{1}{2}m_i\omega_r^2 z_i^2 + \sum_i U_{el}^{(1)}(z_i) + \frac{1}{2}\sum_{i\neq j} U_{el}^{(2)}(r_{ij}).$$

(11)

Here, p_i, m_r, ω_r and z_i are the effective momentum, mass, frequency and tip position of the ith NAMR, $U_{el}^{(1)}(z_i)$ is the electrostatic potential acting on each individual NAMR and $U_{el}^{(2)}(r_{ij})$ is the electrostatic energy depending on the relative position between NAMRs with $r_{ij} = |z_i - z_j|$. We define new equilibrium positions by

$$m_r\omega_r^2 z_i + \left.\frac{\partial U_{el}^{(1)}}{\partial r_{ij}}\right|_{z=0} z_i + \sum_{i\neq j} \left.\frac{\partial U_{el}^{(2)}}{\partial r_{ij}}\right|_{r=0} (z_i - z_j) = 0.$$

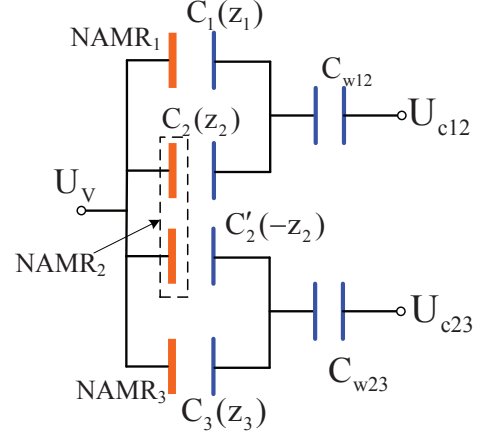(12)

Then the Hamiltonian of these NAMRs can be rewritten

FIG. 7: (Color online.) The equivalent circuit model of coupling switchable NAMRs. Here U_v is the gate voltage applied on each NAMR, $C_i(z_i)$ ($i = 1, 2, 3$) is the capacitance of each NAMR with $C_i(z_i) = C_0(1 - z_i/h)$. For $U_{c12} = U_v$ and $U_{c23} = 0$, there is no energy associated with charge flowing from the gate capacitors onto the wire and thereby the coupling between the first two NAMRs is switched off.

as

$$H_p = \sum_i \frac{p_i^2}{2m_r} + \frac{1}{2}m_r\omega_r^2 z_i^2 + \frac{1}{4}\sum_{i\neq j} K_{ij}(z_i - z_j)^2, \quad (13)$$

with $K_{ij} = \partial^2 U_{el}^{(2)}(r_{ij})/\partial r_{ij}^2$. After quantization, the interaction between these NAMRs can be described by

$$\frac{\hbar}{2}\sum_{ij} g_{ij}(a_i + a_i^\dagger)(a_j + a_j^\dagger), \quad (14)$$

with

$$g_{ij} = z_0^2 K_{i,j}/\hbar, \quad (15)$$

here, $z_0 = \sqrt{\hbar/(2m_r\omega_r)}$.

Now, we drive the expression of $U_{el}^{(2)}$. The equivalent circuit of the model in Fig. 1 is as shown in Fig. 7 for $N = 3$. The equivalent inductance and the equivalent resistance are not shown in this circuit. The NAMRs serve as the left plates of the capacities identified by the red bold line. The capacities of the wires connecting the NAMRs are labeled by C_{w12} and C_{w23}. The voltages U_{c12} and U_{c23} are the coupling control voltages between the first two NAMRs and the last two NAMRs.

In the case of $U_{c12} = U_{c23} = 0$, the electrostatic energy stored in this circuit is

$$U_{el}^{(2)} = \frac{1}{2}(C_{12} + C_{23})U_v^2, \quad (16)$$

with $C_{12}^{-1} = [C_1(z_1) + C_2(z_2)]^{-1} + C_{w12}^{-1}$ and $C_{23}^{-1} = [C_2'(-z_2) + C_3(z_3)]^{-1} + C_{w23}^{-1}$. Therefor the three NAMRs
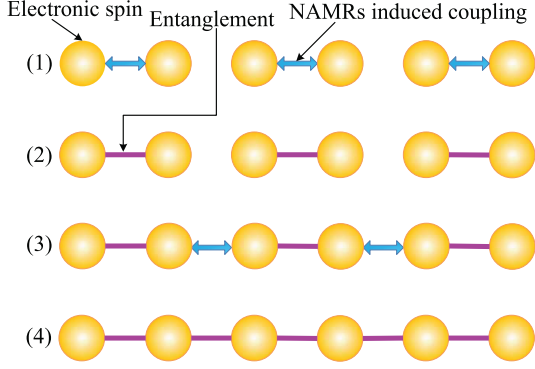
FIG. 8: (Color online.) A sketch for the procedures to compensate for the device errors. Meanwhile, this method can avoid the influences of the effective next-nearest spin-spin couplings.

couples together. When we set the control voltages $U_{c12} = U_v$ and $U_{c23} = 0$, the energy gives

$$U_{el}^{(2)} = \frac{1}{2}C_{12}(U_v - U_{c12})^2 + \frac{1}{2}C_{23}U_v^2 = \frac{1}{2}C_{23}U_v^2. \quad (17)$$

Thus the coupling of the first two NAMRs is switched off. In the two NAMR case, the the expression of g_{ij} can be derived from the equation (15)

$$g = \frac{C_0^2 C_{w23}^2 U_v^2}{(2C_0 + C_{w23})^3} \frac{a_0^2}{h^2}. \quad (18)$$

Here C_0 is a constant with the dimension of capacitance and h is the electrode spacing of the two NAMRs.

B.   Generating entanglement

For simplicity, we assume N is an even number (for an odd N, we only need to regard the last spin as an already entangled spin pair). One can achieve the perfect entanglement through the following procedures as sketched in Fig. 8: (1) switch on the odd-even NAMR nearest couplings and switch off the even-odd NAMR nearest couplings. (2) control the evolution times between each two-spin pair to obtain the maximal entanglement between them and then switch off the coupling, respectively. (3) switch on the even-odd NAMR nearest couplings when all the couplings in (2) are switched off. (4) repeat (2). The total time needed for all these processes is approximately two times of that in the case of no frequency errors.

In our solution, the effective next-nearest spin-spin couplings no longer exist and thus this method avoid their destructiveness. In addition, we should note that the influences of other device errors can also be compensated for since these errors can be reduced to the effective spin-spin coupling errors.

Proof. The operators of different spins communicate with each other. In the case of no errors, the NAMR-spin couplings reduce to a constant and can be denoted by λ. All the effective nearest spin-spin couplings induced by the NAMRs are equal to each other and denoted by M. According to the Ising model, the evolution operator of the spin chain for a given evolution time t_g is:

$$U_g(t_g) = \exp\left\{ i \sum_{i=1}^{N-1} M\sigma_z^i \sigma_z^{i+1} t_g \right\}$$
$$= \prod_{i=1}^{N-1} \exp\left\{ iM\sigma_z^i \sigma_z^{i+1} t_g \right\}. \quad (19)$$

In the case of errors, the NAMR-spin couplings and the collective modes of the NAMRs are shifted by the device errors. Denoting the coupling strength between the ith and $(i+1)^{th}$ spins as $M_{i,i+1}$, the maximal entanglement between two spins can be obtained by adjusting the evolution time in the two spin case as shown in Fig. 6 and the evolution time needed is denoted by $t_{i,i+1}$. When all the four steps are completed (Fig. 8), the evolution operator of these spins can be described by:

$$U_g(t_{1,2} \cdots t_{N-1,N}) = \prod_{i=1}^{N-1} \exp\left\{ iM_{i,i+1}\sigma_z^i \sigma_z^{i+1} t_{i,i+1} \right\}. \quad (20)$$

By precisely controlling the evolution time $t_{i,i+1} = (Mt_g)/M_{i,i+1}$, the evolution operators in the two cases are equal to each other and the two final states must be the same if the system evolutes from the same initial state. □

We should point out that the entanglement of the spins prepared by the following steps is not perfect: (1) switch on all the nearest NAMR-NAMR couplings. (2) switch off the coupling when the nearest spins involute to the maximal entanglement sates, respectively. A spin interacts with all the other spins through the collective modes of the NAMRs when the control voltage is zero. These interactions inevitably include next-nearest interactions and so on. These next-nearest interactions decay as $M_{i,i\pm m} \sim (g/\omega_r)^{m-1}$ [6], but their influences are generally comparable with those due to device errors. Unwanted entanglement between the spins which are not nearest neighbours is generated and the Ising couplings produced by the above two steps is unsatisfactory.

VI.   DISCUSSIONS AND CONCLUSIONS

Although only the one-dimensional case is discussed in the context, the similar analysis on the two-dimensional NAMR-spin quantum computing architecture [6] can also be handled by using the same method. In the two-dimensional configuration, NAMRs are ordered on a two-dimensional lattice and couple to their four neighbours

electrostatically. In the two-dimensional case, the effects of the device errors can be analysed by adjusting the matrix B in equation (10b) to be a general matrix instead of a tridiagonal matrix when considering the nearest couplings. In the compensation method, a switchable voltage gate should be added between each two nearest NAMRs.

In summary, we study the consequence of the next-nearest spin-spin couplings and other device errors on the scalability of the NAMRs-based-on quantum computing architecture. The influences on the quantum operation fidelity are analyzed, and a method is given to compensate for the negative effects of these device errors and void the effective next-nearest spin-spin couplings.

Appendix A: Diagonalizing the quadratic boson Hamiltonian

When the frequencies of the NAMRs are exactly the same (denoted by ω_r) and the nearest NAMR-NAMR coupling is a constant g, the frequencies of collective modes can be obtained by solving the eigenvalue equations analytically and are given by $\widetilde{\omega}_n = \sqrt{\omega_\mathrm{r}^2 + 4\omega_\mathrm{r} g\{1 + \cos[(n+1)\pi]/N\}}$. In practice, the frequencies of all the NAMRs can't be exactly the same due to imperfect fabrications. These frequency errors of each NAMR are independent and are not the same, the frequencies of the collective modes of N coupled NAMRs $\widetilde{\omega}_n$ can't be simply calculated by the perturbation method. A useful method is described as follows.

The Hamiltonian (1) in the context can be rewritten as

$$H_\mathrm{ph} = \hat{\mathbf{a}}^\dagger \mathscr{D} \hat{\mathbf{a}} = \sum_{k=1}^N \widetilde{\omega}_k b_k^\dagger b_k, \tag{A1}$$

with $b_k^\dagger$ (b_k) the creation (annihilation) operators for the phonons of the collective modes and $\hat{\mathbf{a}} \equiv [a_1, \cdots, a_N, a_1^\dagger, \cdots, a_N^\dagger]^T$ the natural creation (annihilation) operators of all the NAMRs. Here $\mathscr{D} = \begin{bmatrix} A & B \\ B & A \end{bmatrix}$, A is an $N \times N$ diagonal real matrix depending on the free Hamiltonian of these NAMRs and B is an $N \times N$ symmetric real matrix governed by the coupling model between NAMRs.

Introducing an auxiliary matrix $D = A^2 - B^2$, the para-values and para-vectors [17] (and also the diagonalizing para-unitary matrix [18]) of $\mathscr{D}$ can be constructed from the eigenvalues (denoted by d_k with $k = 1 \cdots N$) and eigenvectors (denoted by ξ_k) of D [19]. Then the $2N \times 2N$ transformation matrix is given by $J^{-1} \equiv [\zeta_1 \zeta_2 \cdots \zeta_N \zeta_{N+1} \cdots \zeta_{2N}]$ with ζ_k and ζ_{N+k} [20] are $2N$-column vectors [19]. The transformation matrix should satisfy $(J^\dagger)^{-1} \mathscr{D} J^{-1} = \mathrm{diag}(d_1^{1/2}, d_2^{1/2}, \cdots, d_N^{1/2}, d_1^{1/2}, d_2^{1/2}, \cdots, d_N^{1/2})$ to preserve the commutation relations of bosonic operators. The collective frequencies of these NAMRs are

$$\widetilde{\omega}_k = 2 d_k^{1/2}. \tag{A2}$$

By denoting $\hat{\mathbf{b}} = [b_1, \cdots, b_N, b_1^\dagger, \cdots, b_N^\dagger]^T$, we obtain the relation

$$\hat{\mathbf{a}} = J^{-1} \hat{\mathbf{b}}. \tag{A3}$$

[1] J. I. Cirac and P. Zoller, Nature **404**, 579 (2000).
[2] Andrew M. Steane, Phys. Rev. A **68**, 042322 (2003).
[3] Daniel Loss and David P. DiVincenzo, Phys. Rev. A **57**, 120 (1998).
[4] Xin-Qi Li and YiJing Yan, Phys. Rev. B **65**, 205301 (2002).
[5] Xiang Hao and Shiqun Zhu, Phys. Rev. A **76**, 044306 (2007).
[6] P. Rabl, S. J. Kolkowitz, F. H. L. Koppens, J. G. E. Harris, P. Zoller and M. D. Lukin, Nature Physics **6**, 602 (2010).
[7] P. Rabl, P. Cappellaro, M. V. Gurudev Dutt, L. Jiang, J. R. Maze, and M. D. Lukin, Phys. Rev. B **79**, 041302(R) (2009).
[8] Z. Y. Xu, Y. M. Hu, W. L. Yang, M. Feng, and J. F. Du, Phys. Rev. A **80**, 022335 (2009).
[9] Li-gong Zhou, L. F. Wei, Ming Gao, and Xiang-bin Wang, Phys. Rev. A **81**, 042323 (2010).
[10] Eyal Buks and Michael L. Roukes, Journal of Microelectromechanical Systems **11**, 802 (2002).
[11] J. P. Keating, N. Linden, J. C. F. Matthews, and A. Winter, Phys. Rev. A **76**, 012315 (2007).
[12] J. Wrachtrup and F. Jelezko, Journal of Physics: Condensed Matter **18**, S807 (2006).
[13] Hans J. Briegel and Robert Raussendorf, Phys. Rev. Lett. **86**, 910 (2001).
[14] P. B. Li, Y. Gu, Q. H. Gong, and G. C. Guo, Eur. Phys. J. D **55**, 205 (2009).
[15] P. Neumann, N. Mizuochi, F. Rempp, P. Hemmer, H. Watanabe, S. Yamasaki, V. Jacques, T. Gaebel, F. Jelezko and J. Wrachtrup, Science **320**, 1326 (2008).
[16] Torsten Gaebel, Michael Domhan, Iulian Popa, Christoffer Wittmann, Philipp Neumann, Fedor Jelezko, James R. Rabeau, Nikolas Stavrias, Andrew D. Greentree, Steven Prawer, Jan Meijer, Jason Twamley, Philip R. Hemmer, and Jörg Wrachtrup, Nature Physics **2**, 408

(2006).

[17] Para-values and para-vectors. Let $\mathscr{D} = \begin{bmatrix} X & Y \\ Z & W \end{bmatrix}$ with X, Y, Z, W four $N \times N$ matrices. If $\mathscr{D}[u_\rho, v_\rho]^T = \lambda_\rho [u_\rho, -v_\rho]^T$ is stasified, where u_ρ, v_ρ are N-column vectors with $\rho = 1, 2, \cdots, 2N$, we call λ_ρ the para-values and $[u_\rho, v_\rho]^T$ the para-vectors of the matrix $\mathscr{D}$.

[18] Para-unitary matrix. Define the para-unit matrix $\mathscr{I} \equiv \mathrm{diag}(1, 1, \cdots, 1, -1, -1, \cdots, -1)_{2N \times 2N}$. We call $\mathscr{J}$ a $2N \times 2N$ para-unitary matrix if $\mathscr{J}^\dagger \mathscr{I} \mathscr{J} = \mathscr{I}$.

[19] J. H. P. Colpa, Physica **93A**, 327 (1978).

[20] The vectors ζ_k and ζ_{N+k} are given by $\zeta_k = C_k \left[(A + d_k^{1/2} I)\xi_k, -B^\dagger \xi_k \right]^T \equiv [u_k, v_k]^T$, $\zeta_{N+k} = C_{N+k} \left[-B\xi_k, (A + d_k^{1/2} I)\xi_k \right]^T \equiv [u_{N+k}, v_{N+k}]^T$. Here, I is the $N \times N$ unit matrix and C_k, C_{N+k} are determined such that the vectors are para normalized : $u_k^\dagger u_k - v_k^\dagger v_k = 1$ and $u_{N+k}^\dagger u_{N+k} - v_{N+k}^\dagger v_{N+k} = 1$.